



Adsorptive Removal of Volatile Organic Compounds from Industrial Effluent Using Synthesized ZnO-CA Composite Base Adsorbent

Bamigboye Mercy Oluwaseyi ^{1*} , Ayinla Ibrahim Kuranga ¹ , Orimolade Benjamin ¹ ,
Mustapha Ayuba Olanrewaju ¹ , Ojo Olayinka Abosede ² , Jamiu Wasiu ¹ ,
Abdulganiy Aishat A. ¹ , Oba Hameeda Sinmiloluwa ¹ 

¹Department of Industrial Chemistry, Faculty of Physical Sciences, University of Ilorin, Ilorin, Kwara state, Nigeria.

²Department of Animal Production, Fisheries and Aquaculture, Kwara State University, Malete, Kwara State, Nigeria.

Abstract: In this study, a composite adsorbent consisting of ZnO nanoparticles and cellulose acetate nanoparticles was prepared. The composite was extensively characterized through Scanning electron microscopy (SEM), Transmission Electron Microscopy (TEM), Energy Dispersive X-ray Spectroscopy (EDX), and Brunnaeur Emmet Teller analysis (BET). Batch adsorption experiments were carried out to study the effects of concentration of adsorbate (10- 80 mL), dose of adsorbent (0.1 – 1 g), pH(3-13), contact or exposure time (30-180 minutes) and temperature(30 - 70°C) on the removal of benzene and toluene using the synthesized adsorbent. The pseudo-second-order model well described the kinetics of adsorption studied, and Langmuir's isotherm best described the isotherm modeling of the adsorption data. Thermodynamic studies revealed that all the adsorption processes are feasible, endothermic, and spontaneous. The prepared adsorbent is suitable for removing benzene and toluene from wastewater.

Keywords: Cellulose, benzene, toluene, isotherm, adsorption, ZnO-polymer.

Submitted: February 03, 2023. **Accepted:** November 27, 2023.

Cite this: Oluwaseyi BM et al. Adsorptive Removal of Volatile Organic Compounds from Industrial Effluent Using Synthesized ZnO-CA Composite Base Adsorbent. JOTCSA. 2024; 11(1): 189-204.

DOI: <https://doi.org/10.18596/jotcsa.1247149>.

Corresponding author. E-mail: obaleye.mo@unilorin.edu.ng.

1. INTRODUCTION

Nanoparticles exhibit considerably apparent physical, chemical, and biological characteristics when compared with their bulk counterparts. Nanoparticles have become a great subject of interest due to their diverse range and recent applications in numerous fields, including wastewater treatment (1). Several treatment methods have been demonstrated to effectively sequester volatile organic compounds from water. However, an effective and low-cost method based on nanotechnology can be used to decontaminate municipal and domestic wastewater effectively (1). Nano-sized particles have gained much more interest in recent years due to their desirable

properties and applications in different areas, such as catalysts (2), sensors (3, 4), photoelectron devices (5), and highly functional and effective devices (1). These nanomaterials have novel electronic, structural, and thermal properties of high scientific interest in basic and applied fields. One of the unique properties of some nanoparticles is the adsorption of pollutants. Several nanomaterials have adsorbent properties, which depend on the nanomaterial's size. Chemically modified nanomaterials, especially nanoporous materials, have also attracted much attention due to their large surface area (6).

Toluene and benzene are frequently used in industries as organic chemical solvents, for cleaning

machinery, and in other downstream processes. They can seep into groundwater through leakages in pipes and storage tanks and from improper disposal. The US Environmental Protection Agency (EPA) has recognized these substances as primary pollutants with deleterious effects on human health (6). They are also acknowledged as possessing evident carcinogenic characteristics (3). Therefore, removing these hazardous chemical substances from the ecosystem is important for the safety of humans, animals, and aquatic life.

Nanoparticles have become even more crucial as Metal Oxide materials have spread widely throughout human civilization. Due to their intriguing features and wide range of applications, ZnO nanoparticles stand out among them. ZnO nanoparticle production inspired by biological processes has been accomplished utilizing approved ecologically acceptable methods. Numerous studies have examined using natural resources to synthesize ZnO-CA nanoparticles (7), including DNA, silk, albumen, orange juice, pea starch, peptide architectures, and others (4).

Nanoscale metal oxides can increase the effectiveness of technologies and reduce the cost of water treatment due to their small size and high absorption efficiency (3). Therefore, in this study, the adsorption studies of toluene and benzene (8, 9, 10), two prominent volatile organic compounds, were performed using a composite of zinc oxide and cellulose acetate nanocomposites (11). The nanocomposites were fully characterized to ascertain their structural and morphological properties. Additionally, the adsorption process was optimized by studying factors such as adsorbent dose, initial concentration, solution pH affecting adsorption processes, etc (8).

This study aimed to synthesize a composite material using zinc oxide and cellulose acetate derived from agricultural waste and evaluate its adsorption properties/efficiency for the effective removal of benzene and toluene from wastewater. Benzene and toluene, amongst others, are volatile organic compounds commonly found in petroleum-based products, fuels, solvents, and various industrial processes and are considered pollutants and can be harmful to human health and the environment, even at low concentrations (8, 9).

2. MATERIALS AND METHODS

Benzene (anhydrous, 99.8%) and toluene (ACS, 99.7%) were purchased from Sigma Aldrich. ACS (American Chemical Society standards) reagent hydrochloric acid and sodium hydroxide solutions were used for pH adjustment. Zinc Nitrate Hexahydrate salt, Glacial Acetic Acid, Sulfuric acid, and Acetic Anhydride were also acquired from Sigma Aldrich.

2.1. Synthesis of Zinc Oxide Nanoparticles

A method reported by Muneer *et al.* (12) was used with slight modification. Zinc Nitrate Hexahydrate salt (29.785 g) was added to 100 mL 0.1% starch solution to obtain 1 M of zinc nitrate solution. NaOH solution (50 mL, 2M) was added drop-wise along the vessel's walls to the 1 M zinc nitrate solution in a 500 mL beaker while continuously stirring with a magnetic stirrer. The mixture was stirred for 2 hours and filtered through a 0.45 millipore filter paper using vacuum filtration. The paste of zinc hydroxide obtained was washed thrice with distilled water, dried in the oven at 80°C for 5 h, and later calcined in the muffle furnace at 500 °C for 2 h.

2.2. Synthesis of Cellulose Acetate

By procedures described by Okoli *et al.* (13), about 25 g of synthesized cellulose was dispersed in 100 mL of glacial acetic acid. The solution was kept in a water bath at 55 °C for 1 h with frequent stirring. An acetylation mixture of 0.8 mL of concentrated H₂SO₄ and 50 mL of acetic anhydride prepared in a round bottom flask was gradually added to the glacial acetic acid mixture. The resulting solution was kept in a water bath and heated for 2 h with occasional stirring at 55 °C. A clear colloidal solution was obtained, transferred into 1 L of distilled water, and filtered. The residue obtained was oven-dried at 60 °C. The product obtained was characterized using spectroscopic techniques.

2.3. Synthesis of ZnO-CA composites

The composite of ZnO-CA was prepared according to the method prescribed by Patnukao *et al.* (14). This was done at a ratio of 1:1, in which the mixture of each nanomaterial was dispersed in 0.5 M HCl to form a colloidal solution. The solution was stirred and evaporated to dryness in an oven. The composite formed was washed with deionized water, filtered, and further dried in an oven at 100 °C for 12 h and stored in a container.

2.4. Batch Adsorption Experiments

The amount of adsorption (equilibrium concentration) of the adsorbed benzene and toluene, Q_e , was calculated based on the difference between the initial (C_i mg/L) and final concentration (C_e mg/L) of the Benzene and Toluene in solution in every flask after a specified period of shaking, as follows:

$$Q_e = \frac{V(C_i - C_e)}{M} \quad (\text{Eq. 1})$$

Where Q_e = the amount of solute adsorbed out from the solution.

V = Adsorbate Volume,

C_i = the concentration before adsorption,

C_e = the concentration after adsorption, and M = the weight in grams of the adsorbent (15).

2.4.1. Effect of Concentration of Adsorbate

Benzene and Toluene solutions (25 mL) with concentrations ranging from 10 – 80 mg/L were added to different conical flasks. Each adsorbent (0.1 g) was in contact with the solution. Other parameters were kept constant. Then, the mixtures were auto-shook in a flask-shaker at 150 rpm and 25 °C. After that, the flasks were withdrawn, the mixtures filtered, and the absorbance of the solutions measured (16).

2.4.2. Effect of Adsorbent Dose

Different adsorbent doses (0.1, 0.2, 0.3, 0.4, 0.5, and 1 g) were added to each flask, keeping other parameters constant. All the solution flasks were put inside the shaker at 1000 rpm and 25°C for 120 minutes. After 120 minutes, the flasks were retrieved from the shaker, and the benzene and toluene solutions were filtered from the adsorbents using millipore filter paper. The absorbance of each solution was then assessed (17).

2.4.3. Effect of pH

The working solutions (25 mL) were measured into different conical flasks. Using a pH meter, the pH of each of the solutions was adjusted to fall between the range 3 to 13 with 0.1 M HCl/0.1 M NaOH solution. The optimum dose of the adsorbent obtained from the study "EFFECT OF ADSORBENT DOSE" was contacted with each solution in the flask. Then, the flasks were placed inside the shaker for 120 minutes at 1000 rpm and 25°C. The mixtures were filtered, and the absorbance of the filtrate was assessed (18).

2.4.4. Effect of Adsorbent Contact Time

The equilibrium concentration of the benzene and toluene solutions, 25 mL each, was measured in conical flasks. The optimum pH and dose of adsorbent obtained above were set in this experiment. The flasks containing the solutions were

loaded into the shaker at 1000 rpm and 25°C, lasting between 30 and 180 minutes, with the flasks removed at 30-minute intervals and other experiment parameters kept constant. Then, the solutions were filtered, and the absorbance of the solutions was measured. (12).

2.4.5. Effect of Temperature

Several conical flasks were filled with the benzene and toluene solutions at their equilibrium concentration (25 mL each). The optimal adsorbent dosages, contact times, and pH obtained were employed. The temperature ranged from 30 to 70 °C, and the resulting solutions were filtered and subjected to UV spectrophotometric analysis. (18).

3. RESULTS AND DISCUSSION

3.1. Characterisation of Adsorbent

3.1.1. SEM, Scanning Electron Microscopy Analysis

The synthesized cellulose acetate, zinc oxide, and their composites were analyzed by SEM (ThermoFisher Scientific with model number Verios 5 XHR), and the corresponding micrographs obtained at 20,000 and 5,000 magnifications are shown in Figure 1 below. The zinc oxide and cellulose acetate images show that the particles are in aggregated form and also developed many pores, which may have resulted from the adsorbent's large surface area. In Figure 1 (e,f), the zinc oxide particles are encircled by cellulose acetate in the composite materials' SEM scans, showing that the cellulose acetate is firmly embedded with the zinc nanoparticles. The surface of the composite material appeared to be rough and coarse with many pores, which indicates the good performance of good adsorbents. This kind of morphology was also observed in the work reported by Imran *et al.* (20) in removing BTEX (Benzene, Toluene, Ethylbenzene, Xylene) using mango seed.

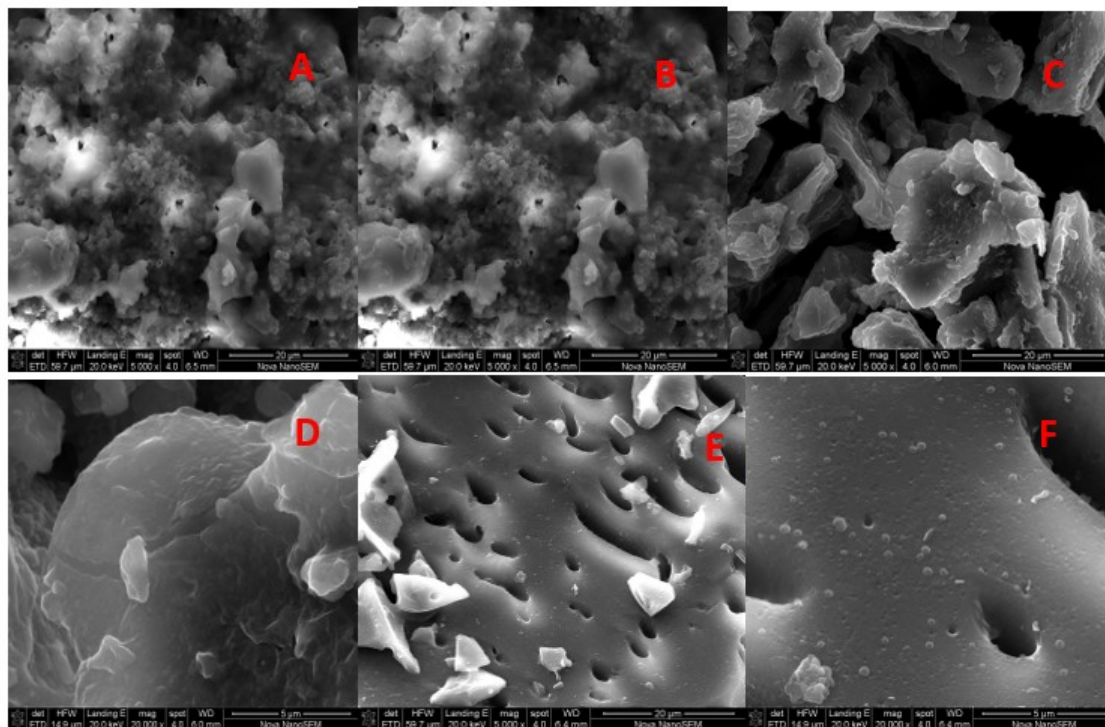


Figure 1: SEM micrograph of (a) ZnO at 20kx (b) ZnO at 5kx. (c) CA at 20kx (d) CA at 5kx. (e) ZnO-CA at 20kx (f) ZnO-CA at 5kx.

3.1.2. Transmission Electron Microscopy Result

The ZnO-CA composite's surface morphology was examined using a transmission electron microscope, Tecnai-12, FEI (Netherlands). As shown in Figure 2, the TEM imaging revealed that the adsorbent material is spherical clusters, which is the characteristic feature of well-defined adsorbents and has been reported to enhance the increase in adsorption properties. The surface covered with micropores showed that the adsorbents developed an elementary pore network, increasing the adsorbents' adsorption properties. In comparing the adsorbents, it can be revealed that the porosity of the surface of the composites observed indicated good adsorption characteristics. By employing CNT and nano iron as adsorbents for removing BTEX from aqueous solutions, Sud *et al.* (21) also noted this trend.

3.1.3. Energy Dispersive X-ray Spectroscopy

Energy Dispersive X-ray Spectroscopy (Shimadzu with Model number: EDX-7200) can be seen from the spectrum Figure 3 (a) that Zn and O show the highest peak, which is predominant, while Si and N are found to be minor elements present. The synthesized ZnO was shown by the spectrum's predominance of Zn and O. From Figure 3 (b), the

presence of Al, C, S, N, and O as predominant elements indicates the presence of agricultural organic raw material used to synthesize cellulose acetate. The presence of Zn, O, and Si in the Figure 3 (c) spectrum shows that the ZnO is well embedded with cellulose acetate. It has been reported that the accuracy of the EDX spectrum can be affected by various factors, which might affect the nature or chemical composition of the adsorbent, and many elements may have overlapping peaks, which would also affect the nature of the sample (22).

3.1.4. Brunauer Emmett Teller (BET)

In this study, the BET of ZnO-CA was measured with a Quantachrome Nova 4200e instrument using the adsorption of N_2 at the liquid nitrogen temperature. The nanocomposite material was determined with a low-temperature adsorption/desorption method based on BET theory multilayer adsorption. The result showed the surface area to be $463.217 \text{ m}^2/\text{g}$, the micropore area to be $414.926 \text{ m}^2/\text{g}$, and the pore volume to be $0.310 \text{ cm}^3/\text{g}$. The BET surface of the material showed that the composite materials possess a high surface area, which is an important requirement for a good adsorbent.

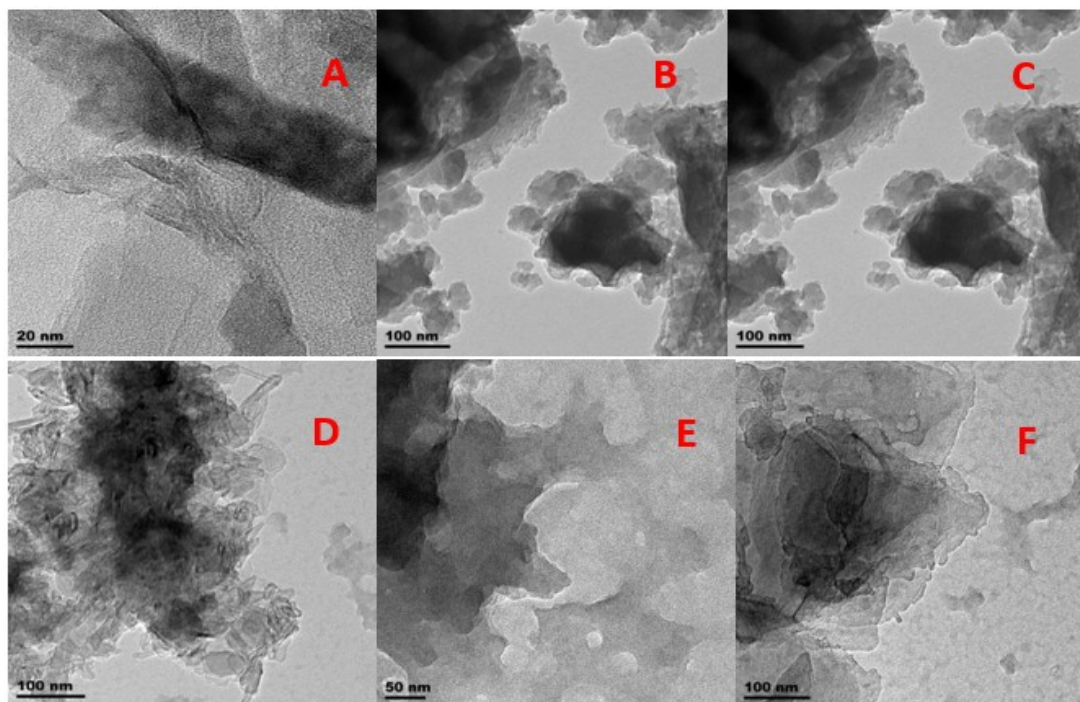


Figure 2: TEM micrographs of (a,b) ZnO nanoparticle (c,d) CA (e,f) ZnO-CA composite.

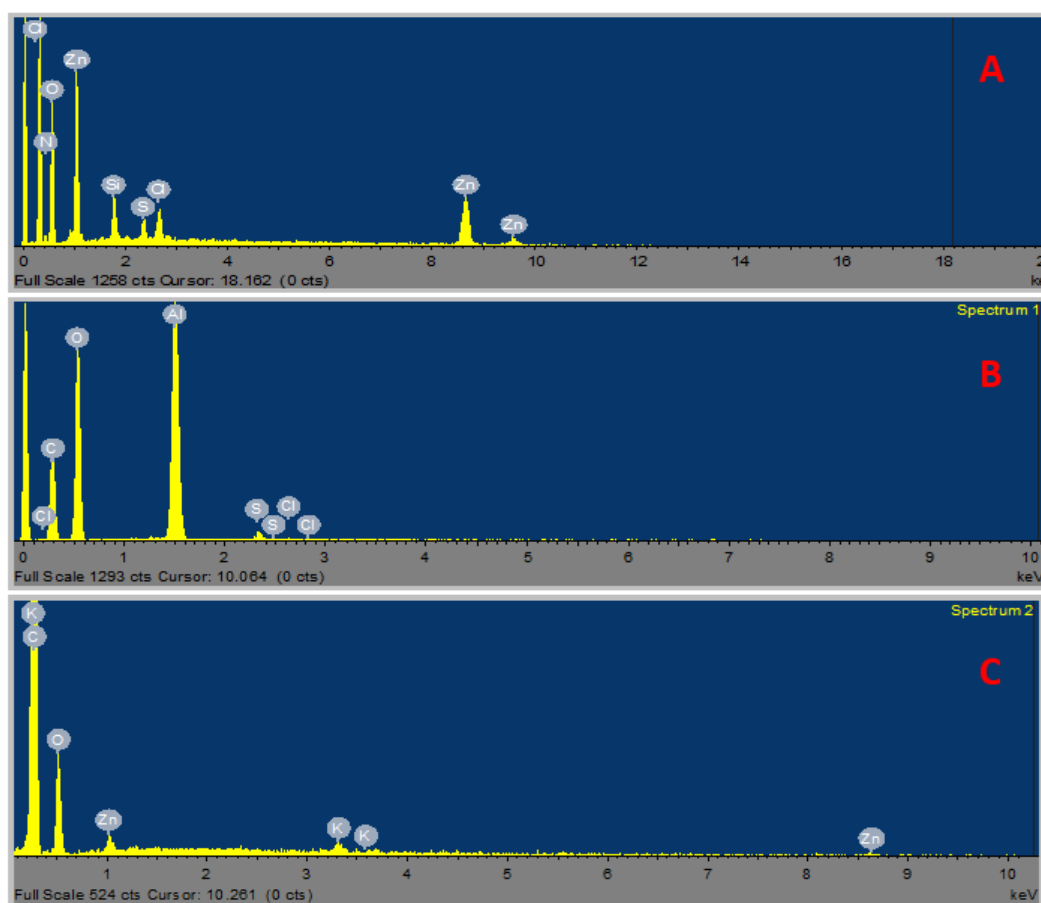


Figure 3: EDX spectra of (a) Zinc Oxide nanoparticle (b) CA (c) ZnO-CA nanocomposites.

3.2 Adsorption Studies Results

By serial dilution of the necessary amounts of the stock, standard working concentrations ranging from 10 to 60 mg/L of benzene and toluene were made from a 1000 mg/L stock solution. A Beckmann Coulter UV-visible spectrophotometer (Searchtech Spectrophotometer with *Model number:752N*) was used to scan the stock solution to determine the maximum wavelength at peak absorbance ($\lambda_{max} = 254$ nm for benzene and 263 nm for toluene). Each dilution of the benzene and toluene was then measured at this maximum wavelength. The absorbances were read and plotted against concentrations to generate the calibration curve. Using extrapolation through the linearity range, the calibration curve was developed from the experimentation and produced the graph equations $y=0.0031x$ for benzene and $y=0.0404x$ for toluene.

3.2.1 Effect of initial concentrations of benzene and toluene

The inception concentration provides a noteworthy impetus to overcome all resistances of mass transfer of solutes between the solid and aqueous phases. In this investigation, initial concentrations of 10-80 mg/L were used to examine the effect of initial concentration on the adsorption of benzene and toluene by ZnO-CA composites, while other parameters like adsorbent dosage, pH, contact time, and temperature were held constant. The result of this effect is displayed below, where the adsorption capacity is plotted against the concentration. In general, this conclusion can be explained by the fact that the ratio of surface active sites to organic molecules is excessively high at low concentrations of benzene and toluene solutions. The species could, therefore, interact with the sorbent to sufficiently occupy the active sites on the adsorbent surface and can be eliminated from the solution (23).

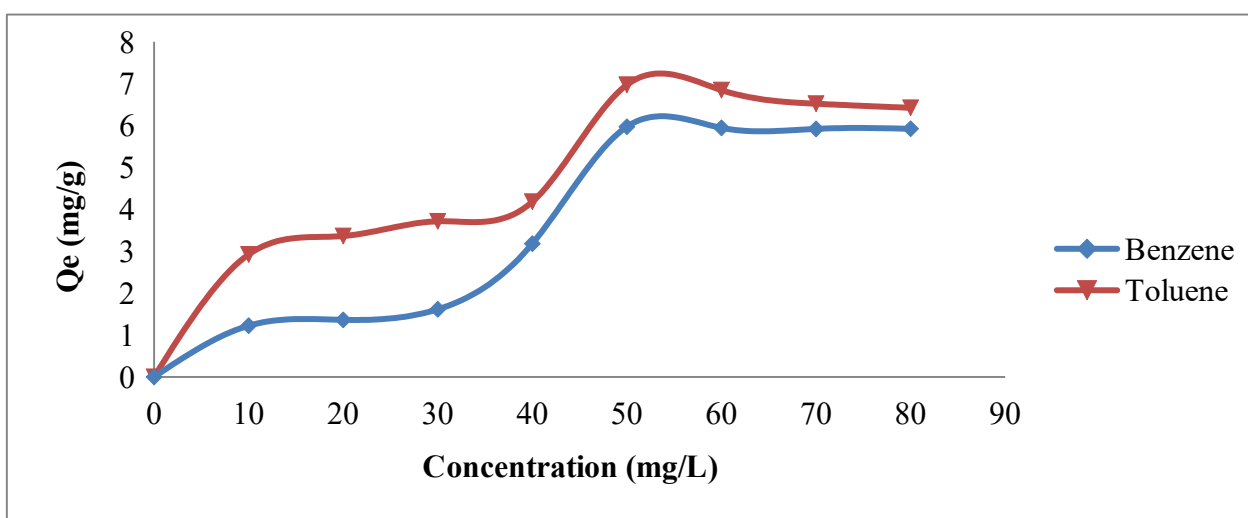


Figure 4: Conc. profile diagram for benzene and toluene adsorption onto ZnO-CA composite (Time: 180 mins, weight of adsorbent: 0.1 g, Temp: 303K, and Volume of adsorbates: 25 mL)

3.2.2. Effect of Adsorbent Dosage

Figure 5 depicts the plot showing the influence of adsorbent dose on the several adsorption systems under investigation. The dosages of the adsorbent ranged from 0.1 g to 1 g. The finding makes it abundantly evident that there was a drop in adsorption equilibrium capacity with an increase in adsorbent dose. This could have arisen from forming aggregates of the adsorbent, thereby limiting the number of sorption sites even after increasing the sorbent dose. A plausibility to this occurrence is that as the mass of the sorbent increases, more sorption

sites are added, but the amount of adsorbate remains constant. This phenomenon is also expressed in equation (1), where the sorption amount is inversely proportional to the adsorbent dose. The observed variation can be explored with pH fluctuations, structural packing (monolayer, cluster, multilayer), etc. In all adsorption systems, the highest adsorption capacity was recorded at 0.1 g, and the corresponding quantities adsorbed for benzene and toluene were 5.826 mg/g and 7.697 mg/g, respectively.

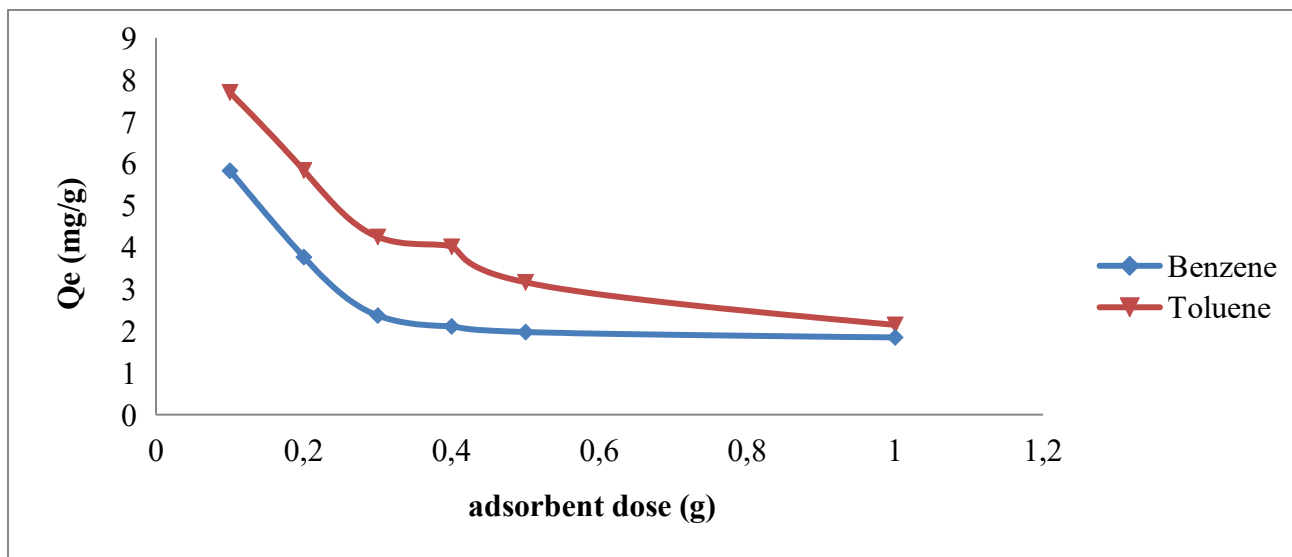


Figure 5: Conc. profile diagram for benzene and toluene adsorption onto ZnO-CA composite (Time: 180 mins, Conc: 50 mg/L, Temp: 303K, and Volume of adsorbates: 25 mL).

3.2.3. Effect of contact/exposure time

Regardless of the other experimental parameters impacting the adsorption kinetics, contact time is crucial in the adsorption system (23). Figure 6 below shows a time profile plot of the adsorption of Benzene and Toluene onto the ZnO-CA composite. The figures show that the amount adsorbed rises

with increasing contact time, reaching equilibrium at 120 minutes for benzene and 90 minutes for toluene, respectively. The maximum amount adsorbed was found for Toluene and Benzene adsorption on the adsorbent, which was 7.773 mg/g and 5.978 mg/g, respectively. The order of adsorption capacity was toluene>benzene.

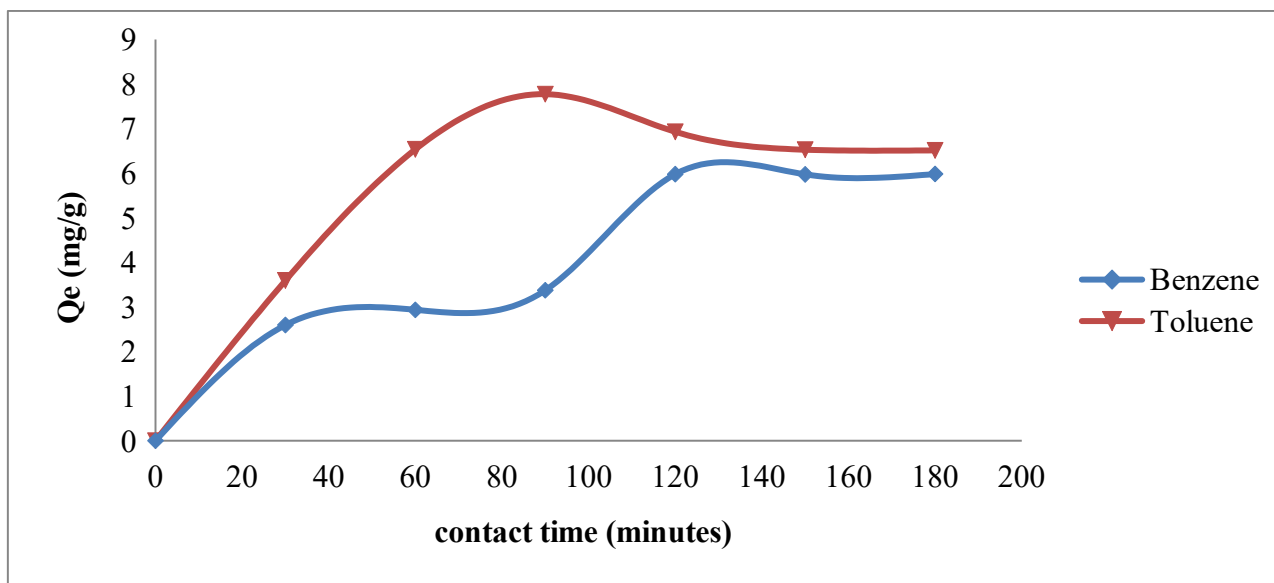


Figure 6: Time profile diagram for benzene and toluene adsorption onto ZnO-CA composite at (Time: 180 mins, Dose: 0.1 g, Conc: 50 mg/L, Temp: 303 K and Volume of adsorbate: 25 mL)

3.2.4. Effect of medium pH

As it affects the solubility of the organic compounds, the concentration of the counter ions on the functional groups of the adsorbent, and the degree of ionization, the initial pH of a solution (Hanna Instruments with Model number: HI2209 pH meter) is a highly significant factor to take into account in adsorption investigations. The plot of this study's

experiment showing the influence of pH on the benzene and toluene adsorption capabilities onto ZnO-CA is presented in Fig. 7. The role of H⁺ concentration was examined from ZnO-CA adsorbent at different pH. The result demonstrates that for both adsorbates, the highest adsorption was noted between pH 5 and 9, with the amount adsorbed increasing as pH increases. Similar

patterns have been documented in other literature (24).

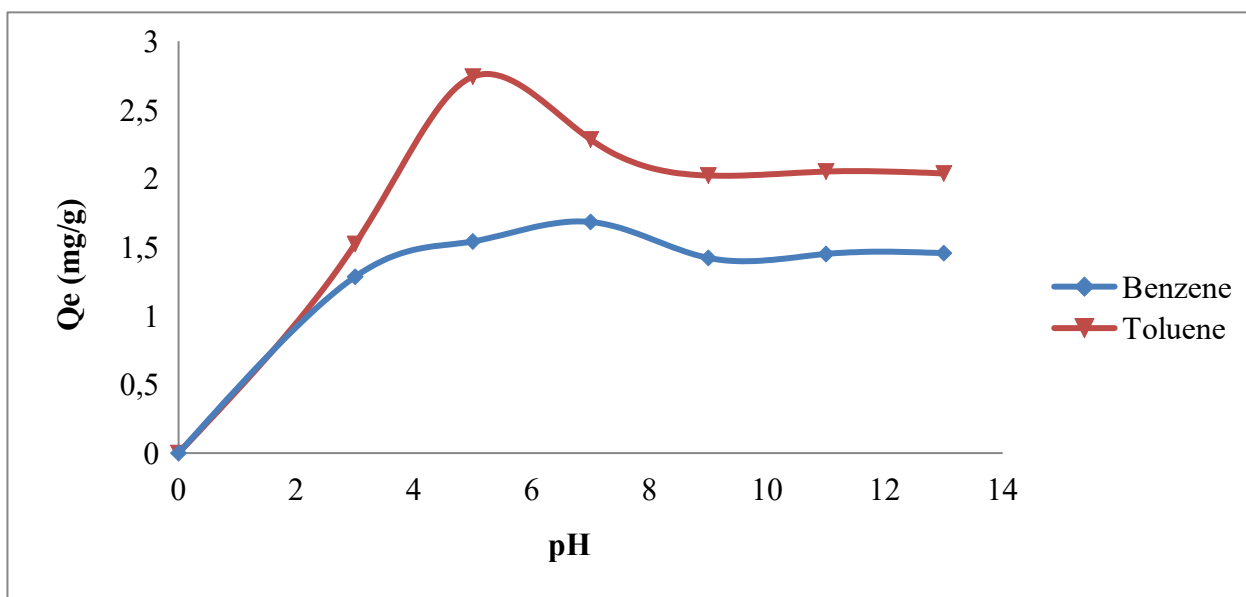


Figure 7: pH profile diagram for benzene and toluene adsorption onto ZnO-CA adsorbent at (Time: 90 & 120 mins, Conc: 50 mg/L, Temp: 303K and Volume of adsorbate: 25 ml).

3.2.5 Effect of Temperature

The temperature is another crucial factor to consider during the adsorption process. The adsorption equilibrium constant and adsorbate solubility are both influenced by temperature (*Japson Thermometer with Model number JD14694*). Five different temperatures (30, 40, 50, 60, and 70 °C) were studied at derived optimized conditions. The adsorption efficiency for benzene and toluene diminishes as the temperature rises, as observed

from the plot of benzene and toluene. This is because higher temperatures cause desorption, which is caused by the loss of volatile molecules and active sites for adsorption (25). The adsorption capacity typically decreases with temperature; the energy content and saturated vapor pressure can explain this behavior. The energy content increases with temperature; therefore, the adsorbent requires more energy to maintain a liquid form, which immediately impacts the adsorption balance.

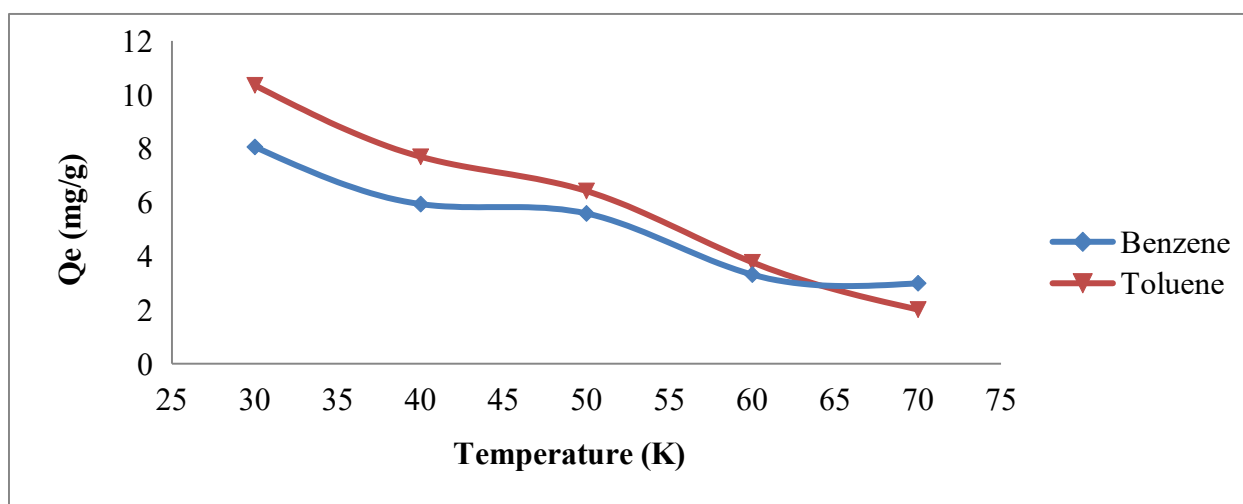


Figure 8: Temperature profile diagram for benzene and toluene adsorption onto ZnO-CA at (Time: 90 & 120 mins, Conc: 50 mg/L, pH: 5, 7 & 9 and Volume of adsorbates: 25 mL).

3.3. Adsorption Isotherm

An adsorption isotherm depicts the relationship between the quantity that has been adsorbed and the amount still in the solution at a certain

temperature and equilibrium. As the adsorption process achieves an equilibrium condition, it describes how the distribution of the liquid phase onto the solid phase occurs (26). The equilibrium

sorption isotherm can be used to determine the adsorbents' performance and adsorption capacity (1). The current study examined the system's adsorption capacity using the Langmuir, Freundlich, and Temkin isotherms model, and plots were displayed.

3.3.1. Langmuir Adsorption Isotherm

For this model, the linearized form of C_e/q_e vs C_e was plotted in Fig. 10, and Table 1 shows the

corresponding constant parameters. The value of R_L specifies whether the adsorption is irreversible if $R_L=0$, unfavorable if $R_L>1$, linear if $R_L=1$, and favorable if $0<R_L<1$. From the information gathered from the plot (Table 1), all of the systems' R_L values are greater than 0 but less than 1, implying that the Langmuir isotherm is favorable for the three systems.

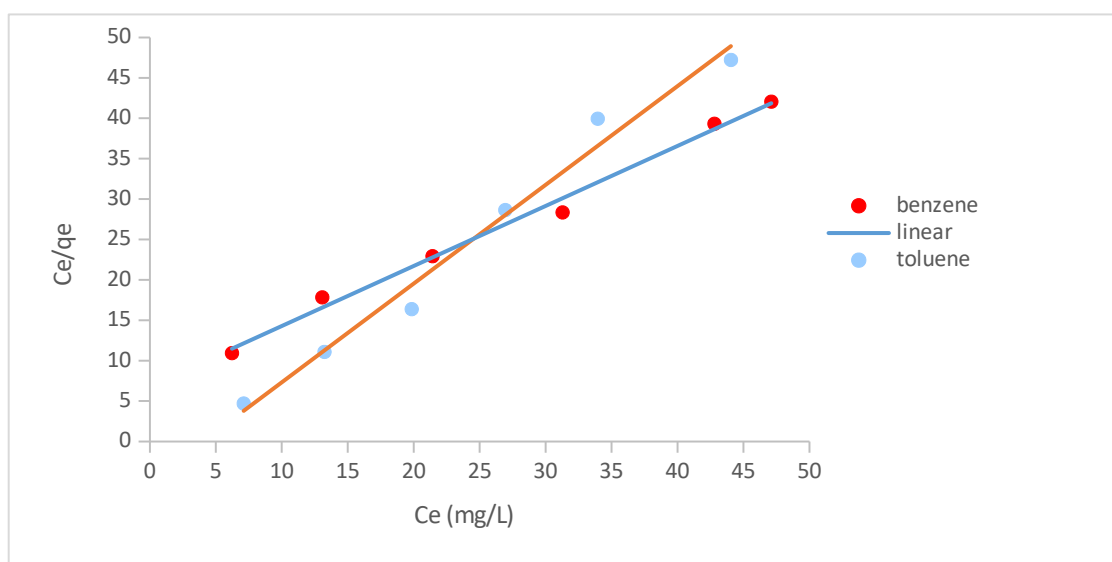


Figure 9: Langmuir isotherm plot of benzene and toluene on ZnO-CA composite.

3.3.2. Freundlich Adsorption Isotherm

For the sorption of benzene and toluene onto ZnO-CA composite, the model's plot of $\log Q_e$ against $\log C_e$ demonstrated linearity, as shown in Fig. 10. From the plot, the regression coefficients and the Freundlich constants n and K_f were deduced. The n values for benzene and toluene are 3.245 and 6.989, respectively, and the regression coefficients R^2 for benzene and toluene onto ZnO-CA composite were 0.932 and 0.401, respectively. These values fall between $1 < n < 10$, indicating that benzene and toluene adsorption onto the ZnO-CA composite is favorable. The values of K_f were calculated to be 0.303 and 0.105. Generally, it can be deduced that the adsorption of Benzene and Toluene was also well fitted to Freundlich adsorption isotherm due to the n value less than 10, except toluene adsorption on to adsorbent, which has a low R^2 value but the adsorption system still favorable.

3.3.3. Temkin Adsorption Isotherm

The model's plot of Q_e against $\ln C_e$ proved linear for the sorption of benzene and toluene onto ZnO-CA, as shown in Fig. 11. From the plot, the K_T , B , and the regression coefficient R^2 were deduced. The calculated K_T values are 2.364 and 2.109, while B values are 0.927 and 0.153; the regression coefficients (R^2) are 0.810 and 0.388 for benzene and toluene, respectively. The higher value of K_T and B indicates a high heat of adsorption and lower binding energy. These low values of binding energies and heat of adsorptions of the adsorption systems indicate physical adsorption (27).

From the isotherm plots and constant parameters, it can be deduced that the data were best fitted into the Langmuir isotherm, and the fitness order is Langmuir>Temkin>Freundlich.

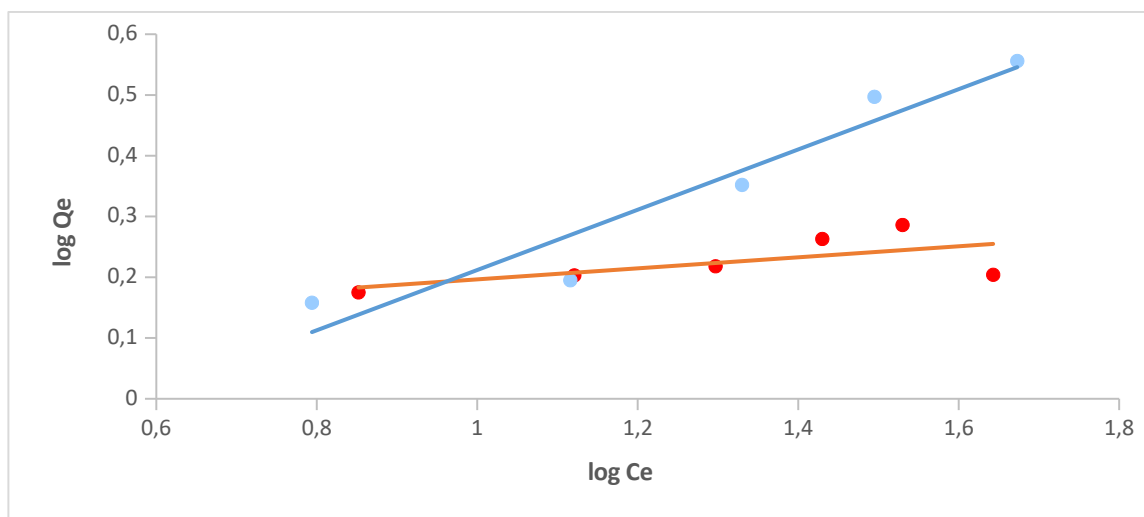


Figure 10: Freundlich isotherm plot for benzene (blue dots) and toluene (red dots) on ZnO-CA composite.

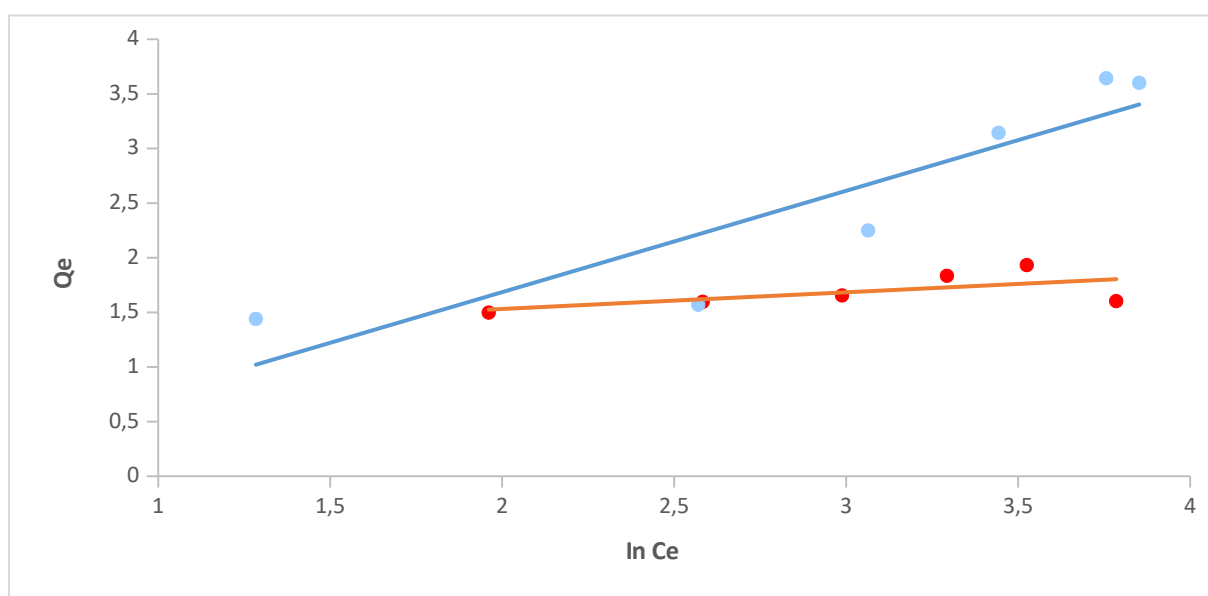


Figure 11: Temkin isotherm plot for benzene (blue dots) and toluene (red dots) on ZnO-CA composite.

Table 1: Isotherm Parameters for Benzene and Toluene Adsorption Systems.

Adsorption Models	Isotherm Parameters	Benzene	Toluene
Langmuir	q_m (mg/g)	5.731	5.358
	K_L (L/mg)	0.063	0.066
	R_L	0.051	0.066
	R^2	0.9926	0.9828
Freundlich	K_f	0.303	0.105
	n	3.245	6.989
	R^2	0.9320	0.4015
Temkin	K_T	2.164	2.219
	B	0.705	0.392
	R^2	0.8107	0.3882

3.4. Adsorption Kinetics

The adsorption rate uptake is very important when designing the adsorption system. The performance of a given adsorbent is of utmost importance to indicate the solute uptake rate. Chemical kinetics covers the factors impacting reaction rate as well as how rapidly chemical reactions happen. It has been noted that system variables, including concentration and temperature, as well as the adsorbent's

physicochemical properties, determine the nature of the adsorption process (28).

3.4.1. Pseudo First Order Kinetic Model

The linearized plot of $\log(q_e - q_t)$ as a function of t was applied to understand the benzene and toluene uptake rate onto ZnO-CA adsorbent. The regression coefficients for the benzene and toluene onto the adsorbent were 0.882 and 0.848, respectively.

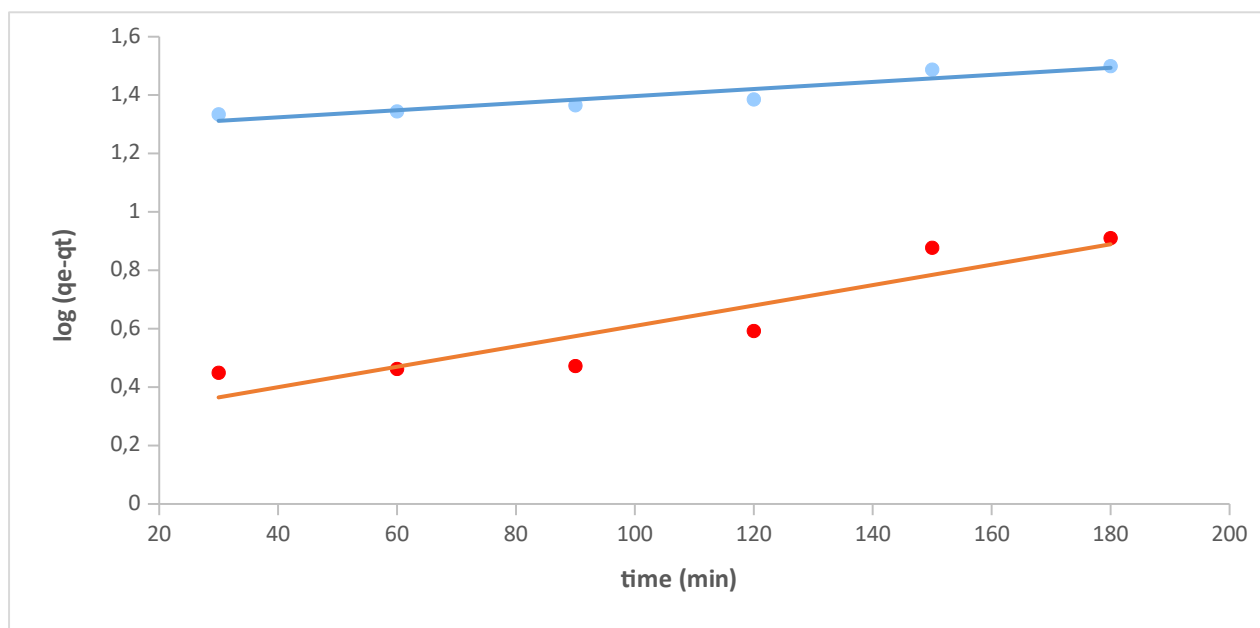


Figure 12: The linear plot of the Pseudo-first order model for benzene (blue dots) and toluene (red dots) onto Zn-CA

3.4.2. Pseudo Second order Kinetic model

Compared to the pseudo-first-order kinetic model, the charts generated for the pseudo-second-order model were more accurate. The pseudo-second-

order kinetic plots, Fig. 13, exhibit superior linearity, with correlation coefficients for benzene and toluene, respectively, of 0.9978 and 0.9888.

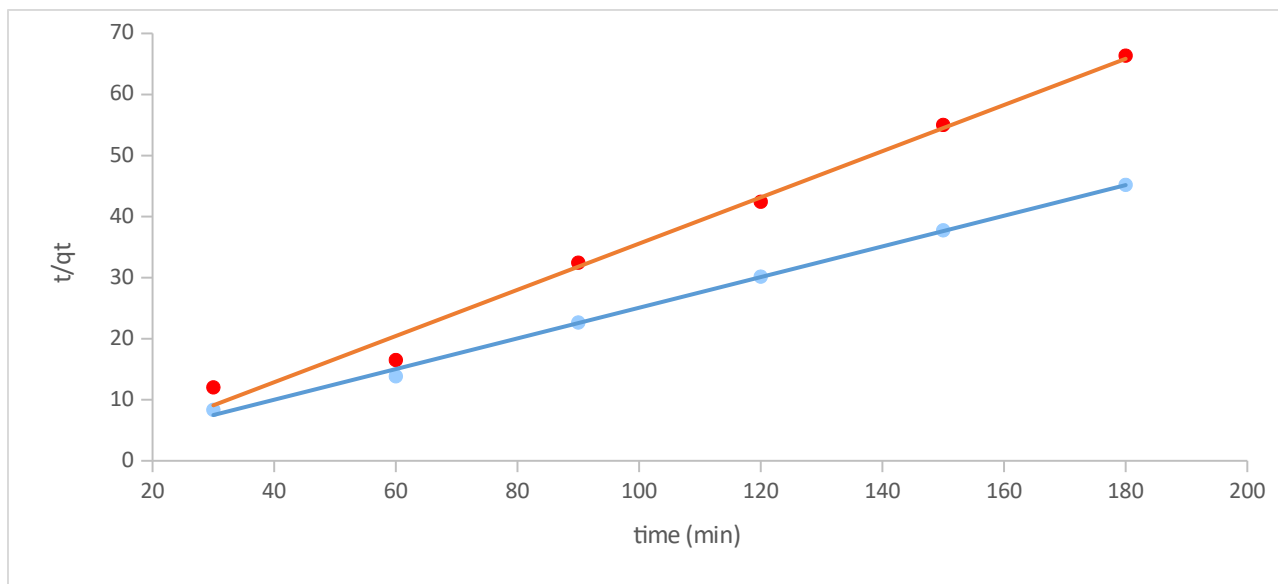


Figure 13: The linear plot of the Pseudo-second order model for benzene (blue dots) and toluene (red dots) onto ZnO-CA.

Table 2: Kinetics Parameters for Benzene and Toluene Adsorption Systems.

Kinetics models	Parameters	Benzene	Toluene
Pseudo-first order	q_e (mg/g)	8.793	1.819
	K_1 (min^{-1})	0.0023	0.0069
	R^2	0.8823	0.8486
Pseudo-second order	q_e (mg/g)	4.684	3.641
	K_2 (min^{-1})	2.423	0.063
	R^2	0.9978	0.9888

3.5. Adsorption Mechanism

The intraparticle diffusion model was used to identify the rate-controlling phases that make up the adsorption mechanism. The diffusion mechanism was depicted using the intraparticle diffusion model. It is widely accepted that the rate is constrained by mass transfer across the boundary layer, and the removal mechanism is difficult if the straight lines from the plots do not travel through the origin (29). At the rate-determining step, the value of constant C provides information about the thickness of the surface adsorption. According to certain reports, the more the pore contributes to adsorption, the larger

the intercept (27). However, the fact that the line in the current investigation did not go through the origin showed that pore diffusion could not be the only process that controls how quickly benzene and toluene are removed, particularly in the early adsorption phases. Due to the great availability of adsorbing sites on the external surface, which becomes the main influence, the surface-adsorbate interaction is thought to control the step rate. The graph of q_t vs $t^{0.5}$ was plotted (Fig. 15), and the intraparticle diffusion constant k_{id} was evaluated from the slope, and the constant C was obtained from the intercept.

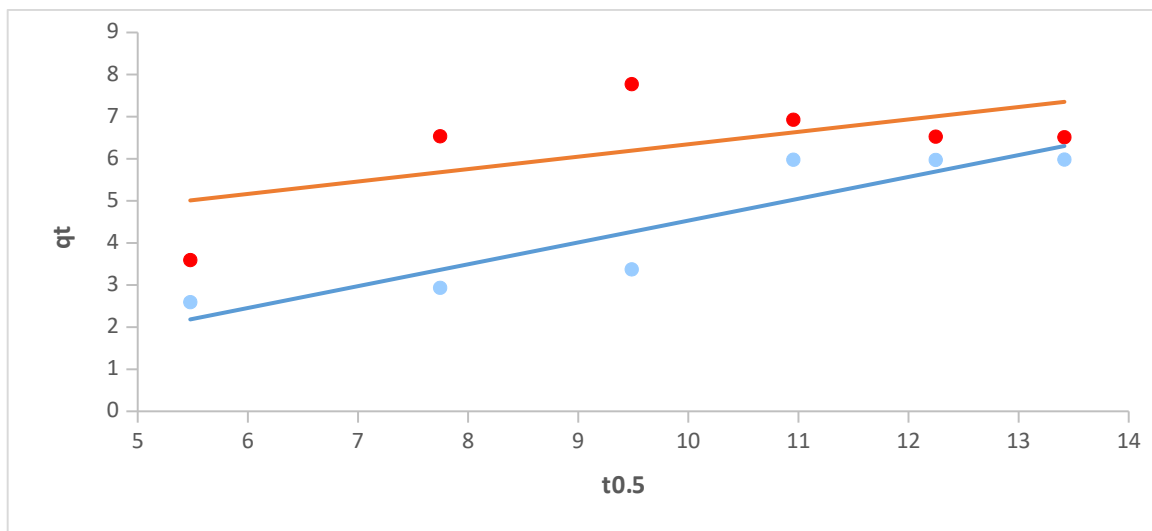


Figure 14: Intraparticle diffusion plot for benzene (blue dots) and toluene (red dots) adsorption on ZnO-CA.

Table 3: Intraparticle diffusion constant parameters for benzene and toluene adsorption.

Adsorbates	$k_{id}(mg/g/min^{0.5})$	C	R ²
Benzene	0.518	0.657	0.839
Toluene	0.295	3.394	0.375
Xylene	1.010	2.855	0.836

3.6. Thermodynamic Studies

The orientation of the physicochemical adsorption reaction, the reaction's viability, and the adsorbed phase's stability can all be evaluated using thermodynamic parameters. The effects of the data from the temperature study were utilized to determine whether the benzene and toluene

adsorption process on the ZnO-CA composite was feasible. Using the relevant equations, the thermodynamic characteristics of the adsorption process, such as the change in enthalpy (ΔH), entropy change (ΔS), and change in Gibbs free energy (ΔG), were calculated for the various systems.

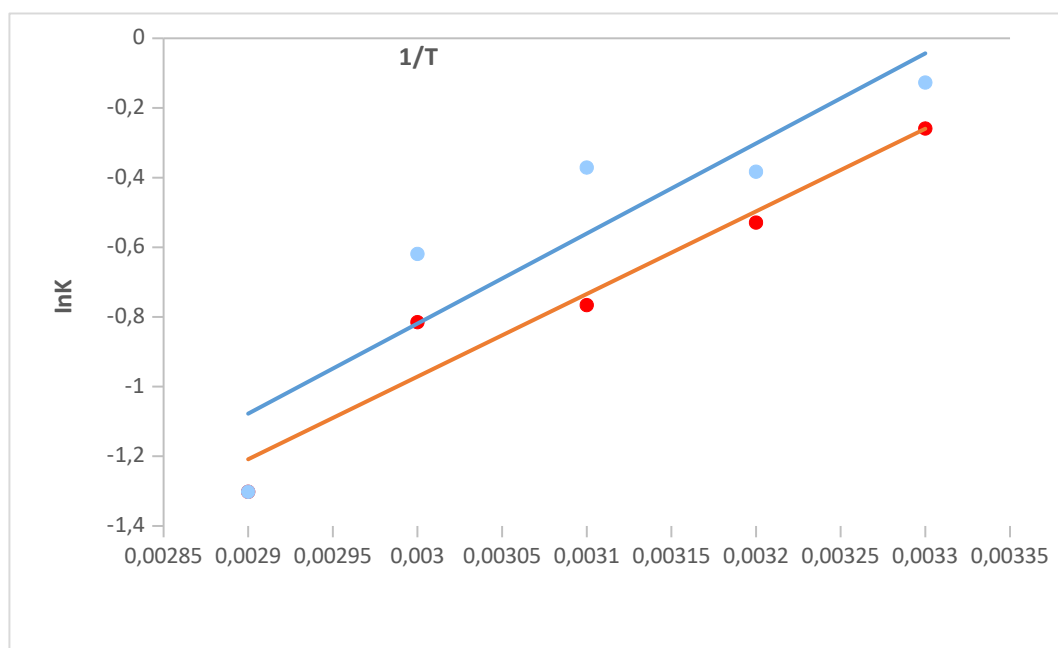


Figure 15: Thermodynamic plot for benzene (blue dots) and toluene (red dots) adsorption on ZnO-CA composite.

Table 4: Thermodynamic parameters for benzene and toluene onto the adsorbent.

Adsorbents	Temperature (K)	ΔG (KJ/mol)	ΔH (KJ/mol)	ΔS (J/mol/K)
BENZENE	303	-31.93		
	313	-99.67		
	323	-99.29	+4951.50	+164.225
	333	-171.73		
	343	-371.91		
TOLUENE	303	-65.45		
	313	-137.60		
	323	-205.03	+4541.02	+154.842
	333	-225.37		
	343	-371.91		

4. CONCLUSION

The synthesis of zinc oxide and cellulose acetate from agricultural waste through the precipitation route was successfully carried out. The composite was formed, and its components were successfully incorporated into each other, as seen in the SEM and TEM images, and were successfully incorporated into each other. The BET surface area, which was evaluated as 463.217 m²/g, demonstrated the adsorbent has good adsorption properties. The batch adsorption experiment result shows that the quantity of benzene and toluene adsorbed depended on the amount of adsorbent dose, initial concentrations of the adsorbate, pH, contact time, and temperature. The Langmuir isotherm best reflected the adsorption data's isotherm modeling of the adsorption kinetics, which the pseudo-second-order model captured well. The value of *n* obtained from Freundlich adsorption parameters indicated favorable adsorption processes. The negative value of Gibb's free energy (ΔG) and positive values of entropy (ΔS) and enthalpy (ΔH) obtained from the thermodynamic studies revealed that all the adsorption processes are feasible, endothermic, and spontaneous. The outcome demonstrated that the adsorbent developed in this study could effectively remove benzene and toluene from wastewater.

The study demonstrates the feasibility and reproducibility of the synthetic process, composite formation, adsorption efficiency, and performance in the sequestration of benzene and toluene from wastewater.

5. CONFLICT OF INTEREST

The authors declare no conflict of interest.

6. ACKNOWLEDGMENTS

We appreciate the effort of the late Professor G.B Adebayo for his contribution and guidance throughout this research work.

7. REFERENCES

1. Badmus MAO, Audu TOK, Anyata BU. Removal of Lead ion from Industrial Waste waters by Activated carbon from Periwinkle shells. *Turkish J Env Sci.* 2007; 31: 251-63.
2. Astruc D. Introduction: Nanoparticles in Catalysis. *Chemical Reviews.* 2020; 120. 461-463. Available from: <URL>.
3. Willner MR, Vikesland PJ. Nanomaterial enabled sensors for environmental contaminants. *J Nanobiotechnol.* 2018; 16: 95. Available from: <URL>.
4. Bueno CC, Garcia PS, Steffens C, Deda DK, de Lima Leite F. *Nanosensors in Micro and Nano Technologies, Nanoscience and its Applications.* 2017; 5:121-153, Available from: ISBN 9780323497800, <URL>.
5. Wang B, Zhu X, Li S, Chen M, Liu N, Yang H, Ran M, Lu H, Yang Y. Enhancing the Photovoltaic Performance of Perovskite Solar Cells Using Plasmonic Au@Pt@Au Core-Shell Nanoparticles. *Nanomaterials (Basel).* 2019 ; 9(9):1263. Available from: <URL>. PMID: 31491914; PMCID: PMC6781053.
6. Jodeh S. The study of kinetics and thermodynamics of selected pharmaceuticals and personal care products on agriculture soil. *Eur J Chemistry.* 2012; 3: 468-74. Available from: <URL>.
7. Chaurasia V, Chand N, Bajpai SK. Water Sorption Properties and Antimicrobial Action of Zinc Oxide Nanoparticles-Loaded Cellulose Acetate Films. *Journal of Macromolecular Science, Part A.* 2010; 47(4): 309-317. <URL>.
8. Alshahrani F, Tawabini B, Saleh T. Removal of benzene, MTBE and toluene from contaminated waters using biochar-based liquid activated carbon. *Sci Rep.* 2022; 12: 19651. Available from: <URL>.
9. George Z K, Gordon M, Tariq J A, Sabereh S, Davoud B. Removal of Benzene and Toluene from Synthetic Wastewater by Adsorption onto Magnetic Zeolitic Imidazole Framework Nanocomposites. *Nanomaterials* 2022; 12(17): 3049. Available from: <URL>.
10. Hirra A, Khairiraihanna J, Nirmala G, Arunagiri A, Murugesan T. Investigation of green functionalization of multiwall carbon nanotubes and its application in adsorption of benzene, toluene & p-xylene from aqueous

- solution. *Journal of Cleaner Production*. 2019. 221: 323-338. Available from: [<URL>](#).
11. Potla D, Rajulapati S.B., Palliparambi A.A. Studies on removal of arsenic using cellulose acetate-zinc oxide nanoparticle mixed matrix membrane. *Int Nano Lett*. 2018; 8, 201-211. Available from: [<URL>](#).
12. Muneer M, Bhatti IA, Adeel S. Removal of Zn, Pb and Cr in textile wastewater using rice husk as a biosorbent. *Asian J Chem*. 2010; 22: 7453 - 59.
13. Okoli J, Ezuma I. Adsorption Studies of Heavy Metals by Low-Cost Adsorbents management. *J Appl Sci Environ Manage*. 2014; 18(3): 443 - 48. Available from: [<URL>](#).
14. Patnukao P, Kongsuwan A, Pavasant P. Batch studies of adsorption of copper and lead on activated carbon from *Eucalyptus camaldulensis* Dehn. *Bark J Environ Sci*. 2008; 20: 1028 -34. Available from: [<URL>](#).
15. Adegoke H, Adekola F. Removal of Phenol from Aqueous Solution by Activated Carbon Prepared from Some Agricultural Materials. *Advances in Natural and Applied Sciences*. 2010; 4(3): 293-98.
16. Radhika V, Subramanian S, Natarajan KA. Bioremediation of zinc using *Desulfotomaculum nigrificans*: Bioprecipitation and characterization studies. *Water Res*. 2006; 40(19): 3628 - 36. Available from: [<URL>](#).
17. Ricordel S, Taha S, Ciss EI, Dorange G. Heavy metals removal by adsorption onto peanut husks carbon: Characterization, kinetic study and modeling *Sep Purif Technol*. 2001; 24(3) : 389- 401. Available from: [<URL>](#).
18. Sheng PX, Ting Y-P, Chen JP, Hong L. Sorption of lead, copper, cadmium, zinc and nickel by marine algal biomass: characterization of biosorptive capacity and investigation of mechanisms. *J Colloid interface Sci*. 2004; 275(1):131-41. Available from: [<URL>](#).
19. Shukla A, Zhang YH, Dubey P, Shukla SS. The role of saw dust in the removal of unwanted materials from water. *J Hazard material*. 2002; 95(12): 137-52. Available from: [<URL>](#).
20. Singh SR, Singh AP. Treatment of water containing chromium (vi) using Rice husk carbon as a new low cost adsorbent. *Int J Environ Res*. 2014; 6(4): 917-924. Available from: [<URL>](#).
21. Sud D, Mahajan G, Kaur MP. Agricultural waste material as potential adsorbent for sequestering heavy metal ions from aqueous solutions- A review. *Biores Techn*. 2008; 99: 6017 - 6027. Available from: [<URL>](#).
22. Joseph G. Scanning Electron Microscopy and X-ray microanalysis. 2003. ISBN 9780-306-47292-3. Retrieved 12 July, 2018
23. Walter GM, Hanna JA, Alen SJ. Treatment of Hazardous Shipyard Wastewater Using Dolomitic Adsorbent. *Wat Res*. 2005; 39(11): 2422 - 28. Available from: [<URL>](#).
24. Wang SB, Boyjoo Y, Choueib A. Zeolitization of fly ash for sorption of dyes in aqueous solutions. *Studies in surf Sci cataly*. 2005; 158 : 161 - 168. Available from: [<URL>](#).
25. Yun J, Choi D, Kim S. Equilibria and dynamics for mixed vapors of BTX in an activated carbon bed, *AIChE J.*, 1999; 45, 751- 60. Available from: [<URL>](#).
26. Thomas JM, Thomas WJ. Introduction to the principles of heterogenous catalysis, 4th edition. Academy Press, New York. 1975; 33-49.
27. Dada AO, Inyibor AA, Oluyori AP. Comparative Adsorption of Dyes onto Activated Carbon Prepared From Maize Stems and Sugar Cane Stems. *IOSR Journal of Applied Chemistry*. 2012; 2(3): 38-43.
28. Adebayo G.B, Adegoke HI, Jamiu W, Balogun BB, Jimoh AA. Adsorption of Mn(II) and Co(II) ions from aqueous solution using Maize cob activated carbon: Kinetics and Thermodynamics Studies. *J Appl Sci Environ Manage*. 2015; 19(4): 737-48. Available from: [<URL>](#).
29. Wiwid PP, Azlan K, Siti NMY, Che FI, Azmi M, Norhayati H, Ilyas MI. Biosorption of Cu(II), Pb(II) and Zn(II) Ions from Aqueous Solutions Using Selected Waste Materials: Adsorption and Characterisation Studies. *J Encap Adsor Sci*. 2014; 4:25. Available from: [<URL>](#).

